






# Broadening the high sensitivity range of squeezing-assisted interferometers by means of two-channel detection

**GAURAV SHUKLA,<sup>1</sup> DARIYA SALYKINA,<sup>2,3</sup> GAETANO FRASCELLA,<sup>4,5</sup>  DEVENDRA KUMAR MISHRA,<sup>1</sup> MARIA V. CHEKHOVA,<sup>4,5</sup>  AND FARIT YA. KHALILI<sup>3,6,\*</sup> **

<sup>1</sup>*Department of Physics, Institute of Science, Banaras Hindu University, Varanasi-221005, India*

<sup>2</sup>*Faculty of Physics, M.V. Lomonosov Moscow State University, 119991 Moscow, Russia*

<sup>3</sup>*Russian Quantum Center, Bolshoy Bulvar 30/bld. 1, 121205 Skolkovo, Moscow, Russia*

<sup>4</sup>*Max Planck Institute for the Science of Light, Staudtstr. 2, 91058 Erlangen, Germany*

<sup>5</sup>*University of Erlangen-Nuremberg, Staudtstr. 7/B2, 91058 Erlangen, Germany*

<sup>6</sup>*UNUST "MISiS", Leninskiy Prospekt 4, 119049 Moscow, Russia*

\**farit.khalili@gmail.com*

**Abstract:** For a squeezing-enhanced linear (so-called SU(2)) interferometer, we theoretically investigate the possibility to broaden the phase range of sub-shot-noise sensitivity. We show that this goal can be achieved by implementing detection in both output ports, with the optimal combination of the detectors outputs. With this modification, the interferometer has the phase sensitivity independent of the interferometer operation point and, similar to the standard dark port regime, is not affected by the laser technical (excess) noise. Provided that each detector is preceded by a phase-sensitive amplifier, this sensitivity could be also tolerant to the detection loss.

© 2020 Optical Society of America under the terms of the [OSA Open Access Publishing Agreement](#)

## 1. Introduction

Optical interferometry has been an efficient tool in a plethora of experiments, starting from the well-known Michelson-Morley's refutation of the ether theory [1] to the high-resolution spectroscopy [2] and to the gravitational-wave detection [3]. The phase sensitivity of the state-of-the-art optical interferometers is limited by the quantum fluctuations of the probing light phase. In the simplest case of a coherent quantum state, the corresponding limit is known as the shot-noise one (SNL):

$$\Delta\phi_{\text{SNL}} = \frac{1}{\sqrt{N}} \quad (1)$$

where  $N$  is the number of quanta used for the measurement (the numerical factor could vary depending on the phase normalization). This sensitivity can be improved by simply increasing the number of photons. However, this may not be an option in biological measurements, where the use of high intensity should be avoided, or in the extremely high precision measurements, where the required optical power is limited by the instabilities and non-linear effects.

Better sensitivity, for the same value of  $N$ , could be achieved using more sophisticated quantum states of light, see *e.g.* the review [4] and the references therein. The first practical scheme of the sub-SNL interferometer, which uses Gaussian squeezed states, created by a degenerate optical parametric amplifier (DOPA), was proposed by Caves in Ref. [5]. Now this idea is implemented in modern laser gravitational-wave detectors GEO-600 [6], Advanced LIGO [7,8], and Advanced VIRGO [9].

Typically in high-power high-precision interferometers, *e.g.* gravitational-wave detectors, one of the interferometer output ports should be tuned to the dark fringe in order to eliminate the

technical noise of the laser and to avoid exposing the photodetector to a high optical power. However, in squeezing-assisted interferometers, this regime limits the range of phases where the high sensitivity is provided [10], while the optical power limitation could be not so significant in smaller-scale (table-top) interferometers.

In Refs. [2,4,11,12], differential detection, with the output signal proportional to the difference of photocurrents of two photodetectors located in both outputs of the interferometer, was considered. However, as we show here, this scheme also has a limited high-sensitivity range.

In this paper, we consider the most universal approach of combining the two photodetector outputs with the optimal weight factors. We show that unlike the dark port regime, this method enables beating the SNL by the same amount regardless of the phase shift in the interferometer (operating point). At the same time, similar to the dark port regime, it is tolerant to the laser technical noise.

The sensitivity gain provided by the squeezed light is limited by the optical losses, both internal (inside the interferometer) and external (absorption in the output path and the detectors inefficiency). A remedy against the detrimental effect of loss has been proposed by Caves in the same paper [5] where squeezing-assisted interferometry was introduced. He showed that the external loss, including the detection inefficiency, can be overcome by amplifying the output signal by a second DOPA before detection. This phase-sensitive amplifier enhances only the quadrature carrying the phase information and thus makes it robust to loss, without introducing additional fundamental noise. This strategy was further analyzed in Ref. [10] and recently implemented in a proof-of-principle experiment [13]. Here, following this approach, we assume that both photodetectors could be preceded by the DOPAs in order to suppress the influence of the photodetectors inefficiency and other external losses.

We base our analysis here on the Mach-Zehnder interferometer topology, but our results could be trivially extended to the Michelson topology as well.

The resulting setup (see Fig. 1) should not be confused with the non-linear so-called SU(1,1) interferometers, which also use the optical parametric amplifiers located before and after the phase shift sources. They measure the phase shift between the parametric pump and the signal beams, with the parametric amplifiers being the core elements of the interferometer. The SU(2)

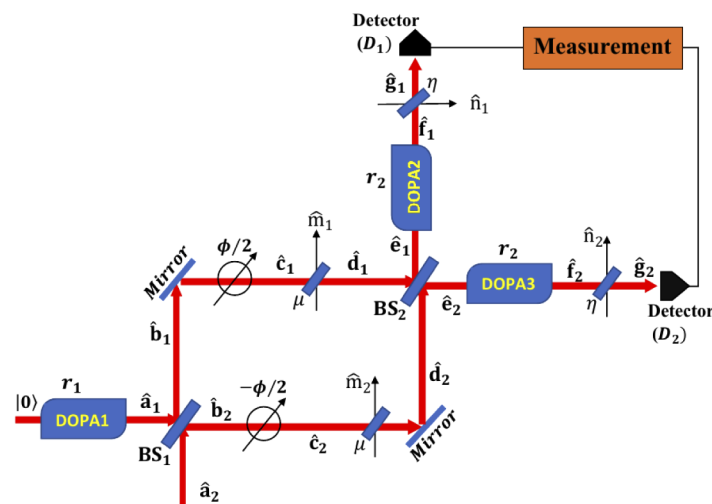


**Fig. 1.** A Mach-Zehnder interferometer with the input degenerate optical parametric amplifiers DOPA1 (the squeezer) and two output ones DOPA2 and DOPA3. The optical losses are represented by the imaginary beamsplitters marked by  $\mu$  and  $\eta$ .

interferometers measure the phase shift between two arms of the interferometer. In this case the parametric amplifiers, while playing the key role in overcoming the SNL, do not participate in the generation of the signal phase shift (see the detailed theory in Ref. [14]).

The paper is organized as follows. In Sec. 2 we derive the input/output equations for this interferometer and find the optimal squeeze angles for all three parametric amplifiers. In Sec. 3 we calculate the optimized sensitivity of this scheme and compare it with the single-detector and differential-detection cases. In Sec. 4 we summarize the obtained results.

## 2. Input/output relations

The specific scheme we consider here is a Mach-Zehnder interferometer with double detection (Fig. 1), which can be viewed as a straightforward extension of the setup used in Ref. [13]. Here squeezed vacuum from an input degenerate optical parametric amplifier DOPA1 is injected into one of the input ports of a Mach-Zehnder interferometer. The second port is fed with the laser radiation. The output signals of the interferometer, which carry the information about the phase shifts in the interferometer arms  $\phi_1$ ,  $\phi_2$ , are amplified by two additional degenerate optical parametric amplifiers DOPA2, DOPA3 and measured by two photodetectors. Finally, the two photocurrents are summed up with the optimal weight factors. In the current paper, we focus on the case of direct detection, as shown in Fig. 1. However, it can be shown that the double detection principle can be extended to the double homodyne detection case as well.

In the case of direct detection, the sum of the phases  $\phi_1 + \phi_2$  is irrelevant. Therefore, we can assume without the generality loss that

$$\phi_1 = -\phi_2 = \frac{\phi}{2}. \quad (2)$$

We assume that our interferometer is a symmetric one, with the reflectivity/transmissivity matrices of both beamsplitters equal to

$$\frac{1}{\sqrt{2}} \begin{pmatrix} 1 & 1 \\ 1 & -1 \end{pmatrix}. \quad (3)$$

We take into account the internal (inside the interferometer) and external (at the interferometer outputs, including the photodetectors inefficiency) loss by introducing imaginary beamsplitters with the power transmissivities, respectively,  $\mu$  and  $\eta$ , which mix the probing light with the vacuum noise, see Fig. 1.

In our calculations, we use the formalism of quadrature amplitudes, which are defined, for any annihilation operator  $\hat{a}$ , as follows [15,16]:

$$\hat{a}^c = \frac{\hat{a} + \hat{a}^\dagger}{\sqrt{2}} \quad \hat{a}^s = \frac{\hat{a} - \hat{a}^\dagger}{i\sqrt{2}}, \quad (4)$$

where the superscripts “c” and “s” denote the cosine and sine quadratures, respectively.

We decompose explicitly the incident laser field in the bright input port into the classical amplitude  $\alpha = \sqrt{N}$  and the noise part  $\hat{z}_2$ :

$$\hat{a}_2 = \alpha + \hat{z}_2, \quad (5)$$

where  $N$  is the mean number of quanta at this port. We assume without generality loss that  $\alpha$  is real. In this case,

$$\hat{a}_2^c = \sqrt{2}\alpha + \hat{z}_2^c, \quad \hat{a}_2^s = \hat{z}_2^s. \quad (6)$$

With an account for this, a straightforward calculation (see *e.g.* [10]) gives the input/output relations for the core part of the interferometer (from the first beamsplitter to the second one, including both of them):

$$\hat{e}_1^c = \delta\hat{e}_1^c, \quad \hat{e}_1^s = \langle\hat{e}_1^s\rangle + \delta\hat{e}_1^s, \quad (7a)$$

$$\hat{e}_2^c = \langle\hat{e}_2^c\rangle + \delta\hat{e}_2^c, \quad \hat{e}_2^s = \delta\hat{e}_2^s, \quad (7b)$$

where

$$\langle\hat{e}_1^s\rangle = \sqrt{2\mu}\alpha \sin \frac{\phi}{2}, \quad \langle\hat{e}_2^c\rangle = \sqrt{2\mu}\alpha \cos \frac{\phi}{2} \quad (8)$$

are the classical components (the mean values) of the respective quadratures,

$$\delta\hat{e}_1^c = \sqrt{\mu}\left(\hat{a}_1^c \cos \frac{\phi}{2} - \hat{z}_2^s \sin \frac{\phi}{2}\right) + \sqrt{1-\mu}\hat{m}_+^c, \quad (9a)$$

$$\delta\hat{e}_1^s = \sqrt{\mu}\left(\hat{a}_1^s \cos \frac{\phi}{2} + \hat{z}_2^c \sin \frac{\phi}{2}\right) + \sqrt{1-\mu}\hat{m}_+^s, \quad (9b)$$

$$\delta\hat{e}_2^c = \sqrt{\mu}\left(-\hat{a}_1^s \sin \frac{\phi}{2} + \hat{z}_2^c \cos \frac{\phi}{2}\right) + \sqrt{1-\mu}\hat{m}_-^c, \quad (9c)$$

$$\delta\hat{e}_2^s = \sqrt{\mu}\left(\hat{a}_1^c \sin \frac{\phi}{2} + \hat{z}_2^s \cos \frac{\phi}{2}\right) + \sqrt{1-\mu}\hat{m}_-^s, \quad (9d)$$

are the noise components with zero mean values,

$$\hat{m}_\pm^{c,s} = \frac{\hat{m}_1^{c,s} \pm \hat{m}_2^{c,s}}{\sqrt{2}}, \quad (10)$$

and  $\hat{a}_{1,2}^{c,s}$ ,  $\hat{e}_{1,2}^{c,s}$ , and  $\hat{m}_{1,2}^{c,s}$  are the quadrature operators of, respectively, the input modes, the output ones, and the vacuum noise modes associated with the internal losses, see notation in Fig. 1.

It follows from Eqs. (7) that the corresponding photon-number operators are

$$\hat{N}_{e1} = \frac{(\hat{e}_1^c)^2 + (\hat{e}_1^s)^2 - 1}{2} = \frac{\langle\hat{e}_1^s\rangle^2}{2} + \langle\hat{e}_1^s\rangle\delta\hat{e}_1^s + \mathcal{O}(\alpha^0), \quad (11a)$$

$$\hat{N}_{e2} = \frac{(\hat{e}_2^c)^2 + (\hat{e}_2^s)^2 - 1}{2} = \frac{\langle\hat{e}_2^c\rangle^2}{2} + \langle\hat{e}_2^c\rangle\delta\hat{e}_2^c + \mathcal{O}(\alpha^0), \quad (11b)$$

where we denoted by  $\mathcal{O}(\alpha^0)$  the small (second-order in quantum fluctuations  $\hat{e}_{1,2}^{c,s}$ ) terms that do not contain  $\alpha$ . In real-world high-precision interferometers, where the number of photons is large,  $\alpha^2 \gg 1$ , these terms can be neglected. In this approximation, the contributions of quadratures  $\hat{e}_1^c$  and  $\hat{e}_2^s$  (which consist of the noise terms only and do not depend on  $\alpha$ ) vanish, giving

$$\hat{N}_{e1} = \frac{\langle\hat{e}_1^s\rangle^2}{2} + \langle\hat{e}_1^s\rangle\delta\hat{e}_1^s, \quad (12a)$$

$$\hat{N}_{e2} = \frac{\langle\hat{e}_2^c\rangle^2}{2} + \langle\hat{e}_2^c\rangle\delta\hat{e}_2^c. \quad (12b)$$

Two conclusions follow from this consideration. First, the quadratures  $\hat{e}_1^s$  and  $\hat{e}_2^c$ , which remain in (12), should be amplified by the output DOPAs to increase the signal. Second, the sine quadrature  $\hat{a}_1^s$ , which appears in Eqs. (9b, 9c), should be squeezed by the input DOPA. This corresponds to the same phases of the pumps of the input DOPA and the second output DOPA, and to the opposite phase of the first output DOPA. Note that these settings do not depend on  $\phi$ .

Taking these assumptions into account, we obtain the following equations for the quadratures  $\hat{g}_1^s, \hat{g}_2^c$  of the effective fields at the photodetectors (with an account for the output losses and the detectors inefficiencies):

$$\hat{g}_1^s = \sqrt{\eta} \hat{e}_1^s e^{r_2} + \sqrt{1-\eta} \hat{n}_1^s = \langle \hat{g}_1^s \rangle + \delta \hat{g}_1^s, \quad (13a)$$

$$\hat{g}_2^c = \sqrt{\eta} \hat{e}_2^c e^{r_2} + \sqrt{1-\eta} \hat{n}_2^c = \langle \hat{g}_2^c \rangle + \delta \hat{g}_2^c, \quad (13b)$$

(note that it is these quadratures that contain the signal and appear in Eqs. (16) below). Here,

$$\langle \hat{g}_1^s \rangle = \sqrt{\eta} \langle \hat{e}_1^s \rangle e^{r_2}, \quad \langle \hat{g}_2^c \rangle = \sqrt{\eta} \langle \hat{e}_2^c \rangle e^{r_2} \quad (14)$$

are the regular parts of  $\hat{g}_1^s, \hat{g}_2^c$ ,

$$\delta \hat{g}_1^s = \sqrt{\eta} \delta \hat{e}_1^s e^{r_2} + \sqrt{1-\eta} \hat{n}_1^s, \quad (15a)$$

$$\delta \hat{g}_2^c = \sqrt{\eta} \delta \hat{e}_2^c e^{r_2} + \sqrt{1-\eta} \hat{n}_2^c \quad (15b)$$

are the noise parts, and  $\hat{n}_1^s, \hat{n}_2^c$  are the quadratures of the vacuum modes associated with the output losses.

### 3. Phase sensitivity

It follows from Eqs. (14, 15) that the effective (accounting for the detectors inefficiency) numbers of detected photons are

$$\hat{N}_1 = \frac{(\hat{g}_1^s)^2}{2} = \langle \hat{N}_1 \rangle + \delta \hat{N}_1, \quad \hat{N}_2 = \frac{(\hat{g}_2^c)^2}{2} = \langle \hat{N}_2 \rangle + \delta \hat{N}_2, \quad (16)$$

where

$$\langle \hat{N}_1 \rangle = \frac{\langle \hat{g}_1^s \rangle^2}{2}, \quad \langle \hat{N}_2 \rangle = \frac{\langle \hat{g}_2^c \rangle^2}{2}, \quad (17)$$

and

$$\delta \hat{N}_1 = \langle \hat{g}_1^s \rangle \delta \hat{g}_1^s, \quad \delta \hat{N}_2 = \langle \hat{g}_2^c \rangle \delta \hat{g}_2^c \quad (18)$$

are the corresponding regular and noise parts.

The explicit expressions for the mean numbers of quanta  $\langle \hat{N}_{1,2} \rangle$ , their variances  $\langle (\delta \hat{N}_{1,2})^2 \rangle$ , the covariance  $\langle \delta \hat{N}_1 \delta \hat{N}_2 \rangle$ , and the corresponding values  $\langle \hat{N}_\pm \rangle$ ,  $\langle (\delta \hat{N}_\pm)^2 \rangle$ ,  $\langle \delta \hat{N}_+ \delta \hat{N}_- \rangle$  for the sum and difference of  $\hat{N}_{1,2}$

$$\hat{N}_\pm = \hat{N}_1 \pm \hat{N}_2 : \quad (19)$$

are calculated in the Appendix A. The following uncertainties of all relevant input quadratures are assumed:

$$\langle (\hat{a}_1^s)^2 \rangle = \frac{e^{-2r_1}}{2}, \quad (20a)$$

$$\langle (\hat{a}_2^c)^2 \rangle = \frac{\mathcal{A}}{2}, \quad (20b)$$

$$\langle (\hat{m}_+^s)^2 \rangle = \langle (\hat{m}_-^c)^2 \rangle = \langle (\hat{n}_1^s)^2 \rangle = \langle (\hat{n}_2^c)^2 \rangle = \frac{1}{2}. \quad (20c)$$

The factor

$$\mathcal{A} = N(g^{(2)} - 1) + 1 > 1 \quad (21)$$

in Eq. (20b), where  $g^{(2)}$  is the degree of second-order coherence, takes into account the contribution from the technical (super-Poissonian) noise of the laser light.

In order to calculate the phase measurement uncertainty, we will use the standard error-propagation formula:

$$(\Delta\phi)^2 = \frac{\langle(\delta\hat{O})^2\rangle}{\left(\frac{\partial\langle\hat{O}\rangle}{\partial\phi}\right)^2}, \quad (22)$$

where  $O$  is the measured quantity.

Consider now three different strategies of the phase measurement.

**Single detector.** The simplest approach is to use just one output, for example the first one:

$$\hat{O} = \hat{N}_1. \quad (23)$$

In this case, Eqs. (47, 48a) give

$$(\Delta\phi)^2 = (\Delta\phi_{\min})^2 + K \tan^2 \frac{\phi}{2}, \quad (24)$$

where

$$\Delta\phi_{\min} = \sqrt{\frac{e^{-2r_1} + \epsilon^2}{N}} \quad (25)$$

is the best sensitivity achieved at  $\phi = 0$ ,

$$K = \frac{\mathcal{A} + \epsilon^2}{N} \quad (26)$$

is the factor describing the sensitivity deterioration with the increase of  $\phi$ , and

$$\epsilon^2 = \frac{1 - \mu}{\mu} + \frac{1 - \eta}{\mu\eta} e^{-2r_2} \quad (27)$$

is the overall quantum inefficiency of the interferometer, compare with Eqs. (5–7) of Ref. [10].

The factor  $K$  defines the range of the phases where the sensitivity is close to  $\Delta\phi_{\min}$ . It follows from Eq. (24) that the full width at half minimum (FWHM) of this range is

$$\Delta_{\text{FWHM}} = 4 \arctan \frac{\Delta\phi_{\min}}{\sqrt{K}} = 4 \arctan \sqrt{\frac{e^{-2r_1} + \epsilon^2}{\mathcal{A} + \epsilon^2}}. \quad (28)$$

It is easy to see that the better the sensitivity, the more narrow the range where it can be achieved. In the most interesting high-sensitivity case of

$$e^{-2r_1} \ll 1, \quad \epsilon^2 \ll 1 \Rightarrow \Delta\phi_{\min} \ll \Delta\phi_{\text{SNL}}, \quad (29)$$

this dependence can be expressed as follows:

$$\Delta_{\text{FWHM}} \approx \frac{4}{\sqrt{\mathcal{A}}} \frac{\Delta\phi_{\min}}{\Delta\phi_{\text{SNL}}}. \quad (30)$$

**Differential detection.** The second possible strategy is to measure the difference of the photon numbers:

$$\hat{O} = \hat{N}_- . \quad (31)$$

It could be justified by the fact that the sum number of quanta  $\hat{N}_+$  does not depend on  $\phi$ , see Eq. (49). In this case it follows from Eqs. (49, 50b) that

$$(\Delta\phi)^2 = (\Delta\phi_{\min})^2 + K \cot^2 \phi. \quad (32)$$

Comparison of this result with Eq. (24) shows that this strategy is not better than the simplest single-detection one, providing the same peak sensitivity and twice as narrow FWHM range

repeated twice in the same phase range  $2\pi$ :

$$\Delta_{\text{FWHM}} = 2 \arctan \frac{\Delta\phi_{\text{min}}}{\sqrt{K}} = 2 \arctan \sqrt{\frac{e^{-2r_1} + \epsilon^2}{\mathcal{A} + \epsilon^2}}, \quad (33)$$

or, in the case of  $\Delta\phi_{\text{min}} \ll 1$ ,

$$\Delta_{\text{FWHM}} \approx \frac{2}{\sqrt{\mathcal{A}}} \frac{\Delta\phi_{\text{min}}}{\Delta\phi_{\text{SNL}}}. \quad (34)$$

**Optimal combination of two output signals.** The best result can be obtained by combining both outputs with some optimized weight factor, which we denote as  $k \pm 1$ :

$$\hat{O} = \hat{N}_k = (k+1)\hat{N}_1 + (k-1)\hat{N}_2 = \hat{N}_- + k\hat{N}_+. \quad (35)$$

Taking into account that  $\hat{N}_+$  does not depend on  $\phi$ , the phase measurement error in this case is

$$(\Delta\phi)^2 = \frac{\langle(\delta\hat{N}_k)^2\rangle}{\left(\frac{\partial\langle\hat{N}_-\rangle}{\partial\phi}\right)^2}. \quad (36)$$

Therefore, the value of  $k$  that minimizes  $\langle(\delta\hat{N}_k)^2\rangle$  provides also the best phase sensitivity. It follows from Eqs. (49–51) that the optimal value of  $k$  and the corresponding value of  $\Delta\phi$  are

$$k_{\text{opt}} = -\frac{\langle\delta\hat{N}_+\delta\hat{N}_-\rangle}{\langle(\delta\hat{N}_+)^2\rangle} = \cos\phi, \quad (37)$$

and

$$\Delta\phi = \Delta\phi_{\text{min}}, \quad (38)$$

compare with Eqs. (24, 32). Thus, the optimal strategy (37) gives a completely flat (independent on  $\phi$ ) value of  $\Delta\phi$ .

At the same time, it creates the “vicious circle”: the factor  $k$  depends on  $\phi$ , which itself is the result of the measurement. Therefore, consider the suboptimal strategy, which uses the following value of  $k$ :

$$k_{\text{subopt}} = \cos\phi_{\text{apr}}, \quad (39)$$

where  $\phi_{\text{apr}}$  is the a priori mean value of  $\phi$ . It follows from Eqs. (49, 51) that in this case,

$$(\Delta\phi)^2 = (\Delta\phi_{\text{min}})^2 + K \frac{(\cos\phi - \cos\phi_{\text{apr}})^2}{\sin^2\phi}. \quad (40)$$

It follows from this equation that in order to obtain good phase sensitivity,  $\Delta\phi \ll 1$ , the deviation of  $\phi_{\text{apr}}$  from the real  $\phi$  also has to be small,

$$\Delta\phi_{\text{apr}} = \sqrt{\langle(\phi_{\text{apr}} - \phi)^2\rangle} \ll 1. \quad (41)$$

However, actually this limitation is rather mild. Indeed, in the case of (41), Eq. (40) can be simplified as follows:

$$(\Delta\phi)^2 = (\Delta\phi_{\text{min}})^2 + K(\Delta\phi_{\text{apr}})^2. \quad (42)$$

Therefore, modest a priori knowledge of  $\phi$ , corresponding to

$$\Delta\phi_{\text{apr}} \lesssim \sqrt{\frac{e^{-2r_1} + \epsilon^2}{\mathcal{A} + \epsilon^2}}, \quad (43)$$

allows one to obtain a sensitivity close to the optimal one (38) for all values of  $\phi$ . Note that the R.H.S. of the above equation does not contain  $N$  and therefore could be much larger than, for example,  $\Delta\phi_{\text{SNL}}$ .

In Fig 2, the phase measurement uncertainties for the considered strategies (24, 32, 38) are plotted as functions of  $\phi$ .

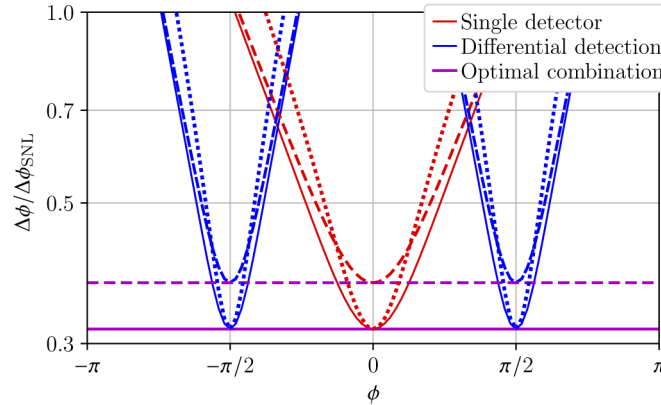


**Fig. 2.** Normalized phase sensitivity for the three considered measurement strategies. Solid lines:  $\epsilon = 0$ ,  $\mathcal{A} = 1$ ; dashed lines:  $\epsilon = 0.2$ ,  $\mathcal{A} = 1$ ; dotted lines:  $\epsilon = 0$ ,  $\mathcal{A} = 2$ . In all cases, 10 dB of the input squeezing is assumed,  $e^{2r_1} = 10$ . (The values of  $\epsilon$  and  $\mathcal{A}$  are chosen with the goal to make clear their influence on the sensitivity).

#### 4. Conclusion

We have analyzed the sensitivity of a Mach-Zehnder interferometer with a squeezed vacuum injected into one of the input ports and the parametric amplification of both output signals, taking into account the optical losses and the detectors inefficiency. We compared three possible strategies of the measurement: (i) measurement of the number of photons at one of the interferometer outputs; (ii) measurement of the difference of photon numbers at both outputs, and (iii) optimal combination of the numbers of photons measured at the two outputs. We showed that while the first two strategies limit the range of phases where the high sensitivity could be achieved, the third one allows to beat the SNL by the same amount for all values of the phase  $\phi$ , assuming some modest a priori information on  $\phi$ . In particular, this information could be acquired using a preliminary low-precision [see Eq. (43)] “ranging” measurement. These results hold independently on whether the output parametric amplification is used or not. However, in all three cases, they allow to suppress the influence of the detectors inefficiency.

It has to be emphasized that the measurement of the photon numbers at both outputs gives the information about the laser intensity noise (which, in linear approximation, is equivalent to the intensity stabilization), allowing to suppress its effect on the measurement precision (note that the factor  $\mathcal{A}$  does not appear in Eq. (38)).

In principle, the DOPAs, both input and output ones, could introduce various non-fundamental imperfections and noise sources into the scheme. The detailed analysis of these effects exceed the framework of the current paper. However, the successful implementation of the squeezing in the GW detectors, as well as the recent demonstration of the sensitivity gain due to the output DOPA [13] show that these problems could be surmounted (see also the brief analysis of the DOPAs losses, which supports this conclusion, in Ref. [17]).

With a broadened range of high phase sensitivity, squeezing-assisted interferometers can improve the performance of many techniques where they have not been used so far. This is, first of all, Fourier-transform infrared (FTIR) spectroscopy, where the phase has to be scanned over ranges exceeding  $2\pi$ . Also, measurements of refractive index, used in various fields from



aerodynamics to environmental gas sensing, are based on the phase shifts in a Mach-Zehnder interferometer and will benefit from broadening its high-sensitivity range.

### A. The photocounting statistics

It follows from Eqs. (14, 20), that

$$\langle g_1^s \rangle = \sqrt{2} G \alpha \sin \frac{\phi}{2}, \quad \langle g_2^c \rangle = \sqrt{2} G \alpha \cos \frac{\phi}{2}, \quad (44)$$

$$\langle (\delta \hat{g}_1^s)^2 \rangle = \frac{G^2}{2} \left( e^{-2r_1} \cos^2 \frac{\phi}{2} + \mathcal{A} \sin^2 \frac{\phi}{2} + \epsilon^2 \right), \quad (45a)$$

$$\langle (\delta \hat{g}_2^c)^2 \rangle = \frac{G^2}{2} \left( e^{-2r_1} \sin^2 \frac{\phi}{2} + \mathcal{A} \cos^2 \frac{\phi}{2} + \epsilon^2 \right), \quad (45b)$$

$$\langle \delta \hat{g}_1^s \delta \hat{g}_2^c \rangle = \frac{G^2}{4} (-e^{-2r_1} + \mathcal{A}) \sin \phi, \quad (45c)$$

where

$$G = \sqrt{\mu\eta} e^{r_2} \quad (46)$$

is the amplitude transfer function of the setup and  $\epsilon^2$  is given by (27). Therefore, with account of Eqs. (17, 18),

$$\langle \hat{N}_1 \rangle = G^2 \alpha^2 \sin^2 \frac{\phi}{2}, \quad \langle \hat{N}_2 \rangle = G^2 \alpha^2 \cos^2 \frac{\phi}{2}, \quad (47)$$

$$\langle (\delta \hat{N}_1)^2 \rangle = G^4 \alpha^2 \sin^2 \frac{\phi}{2} \left( e^{-2r_1} \cos^2 \frac{\phi}{2} + \mathcal{A} \sin^2 \frac{\phi}{2} + \epsilon^2 \right), \quad (48a)$$

$$\langle (\delta \hat{N}_2)^2 \rangle = G^4 \alpha^2 \cos^2 \frac{\phi}{2} \left( e^{-2r_1} \sin^2 \frac{\phi}{2} + \mathcal{A} \cos^2 \frac{\phi}{2} + \epsilon^2 \right), \quad (48b)$$

$$\langle \delta \hat{N}_1 \delta \hat{N}_2 \rangle = \frac{G^4 \alpha^2}{4} (-e^{-2r_1} + \mathcal{A}) \sin^2 \phi \quad (48c)$$

and

$$\langle \hat{N}_+ \rangle = G^2 \alpha^2, \quad \langle \hat{N}_- \rangle = -G^2 \alpha^2 \cos \phi, \quad (49)$$

$$\langle (\delta \hat{N}_+)^2 \rangle = \langle (\delta \hat{N}_1)^2 \rangle + \langle (\delta \hat{N}_2)^2 \rangle + 2 \langle \delta \hat{N}_1 \delta \hat{N}_2 \rangle = G^4 \alpha^2 (\mathcal{A} + \epsilon^2), \quad (50a)$$

$$\langle (\delta \hat{N}_-)^2 \rangle = \langle (\delta \hat{N}_1)^2 \rangle + \langle (\delta \hat{N}_2)^2 \rangle - 2 \langle \delta \hat{N}_1 \delta \hat{N}_2 \rangle = G^4 \alpha^2 (e^{-2r_1} \sin^2 \phi + \mathcal{A} \cos^2 \phi + \epsilon^2), \quad (50b)$$

$$\langle \delta \hat{N}_+ \delta \hat{N}_- \rangle = \langle (\delta \hat{N}_1)^2 \rangle - \langle (\delta \hat{N}_2)^2 \rangle = -G^4 \alpha^2 (\mathcal{A} + \epsilon^2) \cos \phi, \quad (50c)$$

$$\begin{aligned} \langle (\delta \hat{N}_k)^2 \rangle &= \langle (\delta \hat{N}_-)^2 \rangle + 2 \langle \delta \hat{N}_+ \delta \hat{N}_- \rangle \cos \phi_{\text{apr}} + \langle (\delta \hat{N}_+)^2 \rangle \cos^2 \phi_{\text{apr}} \\ &= G^4 \alpha^2 [(e^{-2r_1} + \epsilon^2) \sin^2 \phi + (\mathcal{A} + \epsilon^2) (\cos \phi - \cos \phi_{\text{apr}})^2]. \end{aligned} \quad (51)$$

**Funding.** Russian Science Foundation (20-12-00344); Deutscher Akademischer Austauschdienst (DST/INT/DAAD/P-4/2019); Science and Engineering Research Board, (SERB) New Delhi (EMR/2016/001694); Department of Science and Technology, Ministry of Science and Technology, India (DST/INT/DAAD/P-4/2019).

**Acknowledgments.** DKM and GS acknowledge financial support from DST, Govt. of India. DKM, GS, MC, and GF acknowledge financial support from DAAD, Germany under DST-DAAD joint project (DST/INT/DAAD/P-4/2019). DKM acknowledges financial support under EMR project (EMR/2016/001694) from SERB, New Delhi. FK acknowledges financial support from the Russian Science Foundation (project 20-12-00344).

**Disclosures.** The authors declare no conflicts of interest.

## References

1. A. Michelson and E. Morley, "On the relative motion of the earth and the luminiferous ether," *Am. J. Sci.* **s3-34**(203), 333–345 (1887).
2. U. L. Andersen, O. Gackl, T. Gehring, and G. Leuchs, *Quantum Interferometry with Gaussian States* (John Wiley & Sons, Ltd2019), chap. 35, pp. 777–798.
3. B. Abbott, *et al.*, "Gw150914: The advanced ligo detectors in the era of first discoveries," *Phys. Rev. Lett.* **116**(13), 131103 (2016).
4. R. Demkowicz-Dobrzanski, M. Jarzyna, and J. Kolodynski, "Chapter four - quantum limits in optical interferometry," (Elsevier, 2015), pp. 345–435.
5. C. M. Caves, "Quantum-mechanical noise in an interferometer," *Phys. Rev. D* **23**(8), 1693–1708 (1981).
6. J. Abadie, *et al.*, "A gravitational wave observatory operating beyond the quantum shot-noise limit," *Nat. Phys.* **7**(12), 962–965 (2011).
7. The LIGO Scientific Collaboration, "Enhanced sensitivity of the ligo gravitational wave detector by using squeezed states of light," *Nat. Photonics* **7**(8), 613–619 (2013).
8. M. Tse, H. Yu, N. Kijbunchoo, A. Fernandez-Galiana, P. Dupej, L. Barsotti, C. D. Blair, D. D. Brown, S. E. Dwyer, A. Effler, M. Evans, P. Fritschel, V. V. Frolov, A. C. Green, G. L. Mansell, F. Matichard, N. Mavalvala, D. E. McClelland, L. McCuller, T. McRae, J. Miller, A. Mullavey, E. Oelker, I. Y. Phinney, D. Sigg, B. J. J. Slagmolen, T. Vo, R. L. Ward, C. Whittle, R. Abbott, C. Adams, R. X. Adhikari, A. Ananyeva, S. Appert, K. Arai, J. S. Areeda, Y. Asali, S. M. Aston, C. Austin, A. M. Baer, M. Ball, S. W. Ballmer, S. Banagiri, D. Barker, J. Bartlett, B. K. Berger, J. Betzwieser, D. Bhattacharjee, G. Billingsley, S. Biscans, R. M. Blair, N. Bode, P. Booker, R. Bork, A. Bramley, A. F. Brooks, A. Buikema, C. Cahillane, K. C. Cannon, X. Chen, A. A. Ciobanu, F. Clara, S. J. Cooper, K. R. Corley, S. T. Countryman, P. B. Covas, D. C. Coyne, L. E. H. Datrier, D. Davis, C. Di Fronzo, J. C. Driggers, T. Etzel, T. M. Evans, J. Feicht, P. Fulda, M. Fyffe, J. A. Giaime, K. D. Giardina, P. Godwin, E. Goetz, S. Gras, C. Gray, R. Gray, A. Gupta, E. K. Gustafson, R. Gustafson, J. Hanks, J. Hanson, T. Hardwick, R. K. Hasskew, M. C. Heintze, A. F. Helmling-Cornell, N. A. Holland, J. D. Jones, S. Kandhasamy, S. Karki, M. Kasprzack, K. Kawabe, P. J. King, J. S. Kissel, R. Kumar, M. Landry, B. B. Lane, B. Lantz, M. Laxen, Y. K. Lecoeuche, J. Leviton, J. Liu, M. Lormand, A. P. Lundgren, R. Macas, M. MacInnis, D. M. Macleod, S. Márka, Z. Márka, D. V. Martynov, K. Mason, T. J. Massinger, R. McCarthy, S. McCormick, J. McIver, G. Mendell, K. Merfeld, E. L. Merilh, F. Meylahn, T. Mistry, R. Mittleman, G. Moreno, C. M. Mow-Lowry, S. Mozzon, T. J. N. Nelson, P. Nguyen, L. K. Nuttall, J. Oberling, R. J. Oram, B. O'Reilly, C. Osthelder, D. J. Ottaway, H. Overmier, J. R. Palamos, W. Parker, E. Payne, A. Pele, C. J. Perez, M. Pirello, H. Radkins, K. E. Ramirez, J. W. Richardson, K. Riles, N. A. Robertson, J. G. Rollins, C. L. Romel, J. H. Romie, M. P. Ross, K. Ryan, T. Sadecki, E. J. Sanchez, L. E. Sanchez, T. R. Saravanan, R. L. Savage, D. Schaeztl, R. Schnabel, R. M. S. Schofield, E. Schwartz, D. Sellers, T. J. Shaffer, J. R. Smith, S. Soni, B. Sorazu, A. P. Spencer, K. A. Strain, L. Sun, M. J. Szczepańczyk, M. Thomas, P. Thomas, K. A. Thorne, K. Toland, C. I. Torrie, G. Traylor, A. L. Urban, G. Vajente, G. Valdes, D. C. Vander-Hyde, P. J. Veitch, K. Venkateswara, G. Venugopalan, A. D. Viets, C. Vorvick, M. Wade, J. Warner, B. Weaver, R. Weiss, B. Willke, C. C. Wipf, L. Xiao, H. Yamamoto, M. J. Yap, H. Yu, L. Zhang, M. E. Zucker, and J. Zweizig, "Quantum-enhanced advanced LIGO detectors in the era of gravitational-wave astronomy," *Phys. Rev. Lett.* **123**(23), 231107 (2019).
9. VIRGO Collaboration, "Increasing the astrophysical reach of the advanced VIRGO detector via the application of squeezed vacuum states of light," *Phys. Rev. Lett.* **123**(23), 231108 (2019).
10. M. Manceau, F. Khalili, and M. Chekhova, "Improving the phase super-sensitivity of squeezing-assisted interferometers by squeeze factor unbalancing," *New J. Phys.* **19**(1), 013014 (2017).
11. B. T. Gard, C. You, D. K. Mishra, R. Singh, H. Lee, T. R. Corbitt, and J. P. Dowling, "Nearly optimal measurement schemes in a noisy Mach-Zehnder interferometer with coherent and squeezed vacuum," *EPJ Quantum Technol.* **4**(1), 4 (2017).
12. S. Ataman, A. Preda, and R. Ionicioiu, "Phase sensitivity of a Mach-Zehnder interferometer with single-intensity and difference-intensity detection," *Phys. Rev. A* **98**(4), 043856 (2018).
13. G. Frascella, S. Agne, F. Y. Khalili, and M. V. Chekhova, "Overcoming detection losses in squeezing-assisted interferometers," ArXiv:2005.08843 (2020).
14. B. Yurke, S. L. McCall, and J. R. Klauder, "SU(2) and SU(1,1) interferometers," *Phys. Rev. A* **33**(6), 4033–4054 (1986).
15. C. M. Caves and B. L. Schumaker, "New formalism for two-photon quantum optics. i. quadrature phases and squeezed states," *Phys. Rev. A* **31**(5), 3068–3092 (1985).
16. B. L. Schumaker and C. M. Caves, "New formalism for two-photon quantum optics. ii. mathematical foundation and compact notation," *Phys. Rev. A* **31**(5), 3093–3111 (1985).
17. E. Knyazev, K. Spasibko, F. Khalili, and M. Chekhova, "Quantum tomography enhanced through parametric amplification," *New J. Phys.* **20**(1), 013005 (2018).